Miniaturized Top-Metallized Rectangular Dielectric Resonator Antenna

Mario Pérez-Escribano[(1)], Francisco Javier Herraiz-Martínez[(2)] and Enrique Márquez-Segura[(3)]
mpe@ic.uma.es[(1)], fjherraiz@icai.comillas.edu[(2)], ems@ic.uma.es[(3)]
[(1)(3)]Dpto. de Ingeniería de Comunicaciones, E.T.S. Ingeniería de Telecomunicación, Universidad de Málaga
Campus de Teatinos s/n, E-29071 Málaga (Spain)
[(2)]Instituto de Investigación Tecnológica, Escuela Técnica Superior de Ingeniería ICAI, Universidad Pontificia Comillas
E-28015 Madrid (Spain)

***Abstract*—In this paper, a modal analysis of a rectangular dielectric resonator antenna (DRA), with unconventional boundary conditions, is carried out. Analytical equations of the fields inside the resonator and simulations are presented, showing that if a resonator is mounted over a ground plane and loaded by a top metallic sheet, there is a miniaturization of the electric size of the new antenna, without significant deterioration of performance. Furthermore, dual-band responses can be achieved with this configuration.**

I. Introduction

The current trend of electronic devices is to be smaller, because they are usually made to be transported, carried in a pocket, or even integrated into other objects such as clothing or medical systems [1], [2]. The need of designing compact devices, which requires the miniaturization of the antennas' size, makes that a lot of researches are focused on reducing the size of antennas [3], [4]. In addition to it, the use of multi-band antennas in communication systems for multiple standards is a crucial factor when transporting these devices [5], [6].

High-permittivity dielectric material has been used in microwave circuits such as filters or oscillators [7]. Since the beginning of the 80s, dielectric resonators have been used as antenna elements by exciting different modes of DR using conventional feeding mechanisms [8]. The use of this kind of antennas is due to their known benefits: size of the DRA is proportional to $\lambda_0/\sqrt{\varepsilon_r}$, high radiation efficiency when a low-loss dielectric material is chosen, several possibilities of excitation, etc.

In this paper, the main objective is the development of a new type of DRA in which new modes appear due to the metallization of the ground plane and the upper face. First of all, the cavity model of the proposed antenna has been analytically computed to obtain the electromagnetic fields distribution inside the antenna. The results are corroborated with a complete full-wave simulation.

In section II the geometry is described and a complete modal analysis is performed from the cavity model. In the third section, an antenna model is proposed and the theoretical results are assessed using an electromagnetic simulation tool. Conclusions are shown in the last section.

II. Modal analysis

To design a DRA, it is necessary to use high permittivity materials as mention above, typically $\varepsilon_r > 10$. For this reason,

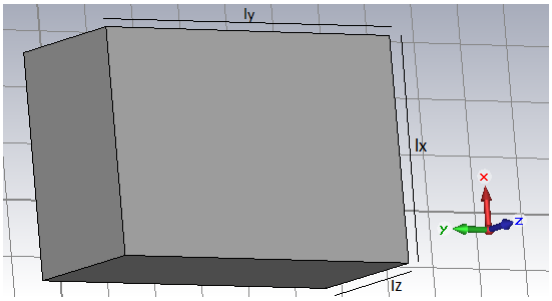

Fig. 1. Geometry of the analysed resonator.

the resonator analysed in this paper is made of Kyocera SB350 (with relative constant $\varepsilon_r = 35$ and $\tan\delta = 8 \cdot 10^{-5}$). A schematic, including the dimensions of each edge ($l_x = 8$ mm, $l_y = 12$ mm and $l_z = 5$ mm respectively) is shown Fig. 1. As z is the smallest dimension of the structure, it can be considered that it is going to be the propagation direction and, therefore, TE^z modes are the first ones to be excited. In order to analyse the proposed DRA, the conventional antenna on a ground plane is considered first, and then, the performance of the metallized prototype is studied.

A. Resonator on ground plane

To perform the analysis, the ground plane is considered as a Perfect Electric Conductor (PEC) and the rest of the walls, Perfect Magnetic Conductors (PMC) [9]. Therefore, the boundary conditions can be expressed as

$$E_z(x=0, 0\le y\le l_y, 0\le z\le l_z) = 0, \tag{1a}$$
$$E_y(x=0, 0\le y\le l_y, 0\le z\le l_z) = 0, \tag{1b}$$
$$H_x(0\le x\le l_x, y=0, 0\le z\le l_z) = 0, \tag{1c}$$
$$H_x(0\le x\le l_x, y=l_y, 0\le z\le l_z) = 0, \tag{1d}$$
$$H_y(x=l_x, 0\le y\le l_y, 0\le z\le l_z) = 0. \tag{1e}$$

and the vector potential F_z^+ is

$$F_z^+ = A_{mn}\cos(\beta_x x)\sin(\beta_y y)e^{-j\beta_z z}, \tag{2}$$

where

$$\beta_x = \frac{(2m+1)\pi}{2l_x}, \tag{3a}$$
$$\beta_y = \frac{n\pi}{l_y}. \tag{3b}$$

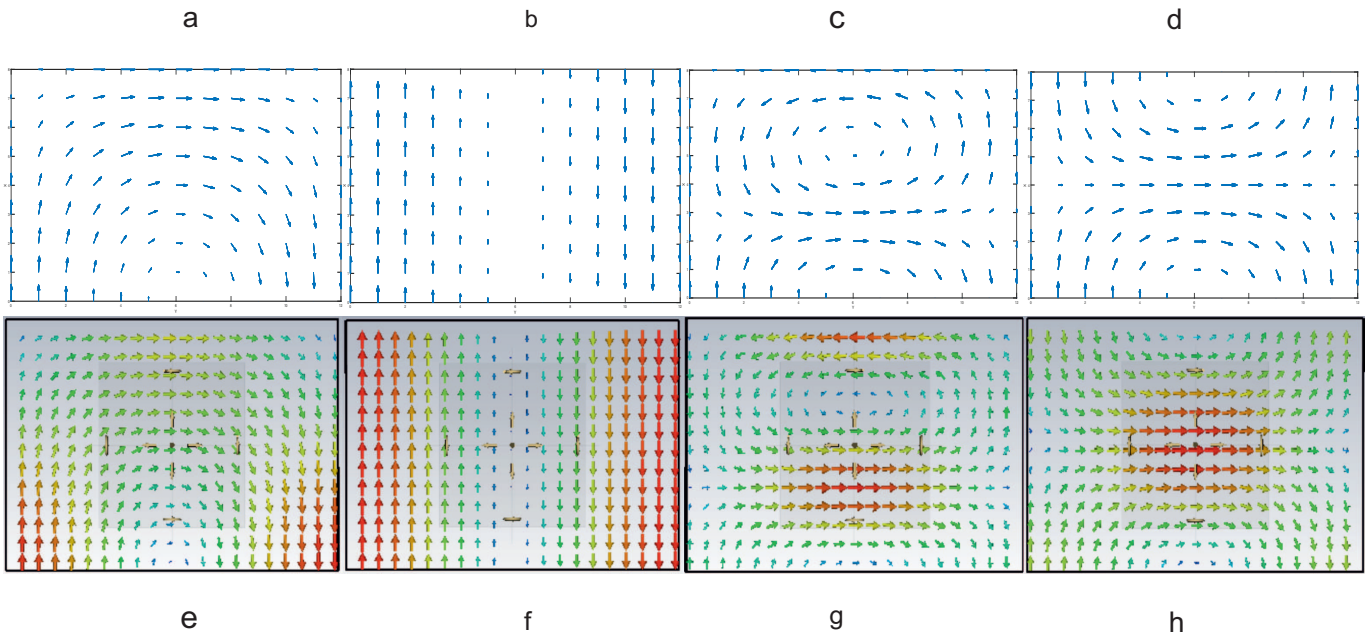

Fig. 2. Electric fields inside the resonator: (a) analytical and conventional TE_{01} mode, (b) analytical and metallized TE_{01} mode, (c) analytical and conventional TE_{11} mode, (d) analytical and metallized TE_{11} mode, (e) simulated and conventional TE_{01} mode, (f) simulated and metallized TE_{01} mode, (g) simulated and conventional TE_{11} mode, (h) simulated and metallized TE_{11} mode.

In this case, *m* can take values 0,1,2,3 ... whereas *n* can take values 1,2,3... Electric and magnetic fields inside the resonator, obtained applying boundary conditions to (2), are given by

$$E_x = \frac{-1}{\varepsilon} A_{mn} \cos(\beta_x x)\beta_y \cos(\beta_y y) e^{-j\beta_z z}, \tag{4a}$$

$$E_y = \frac{-1}{\varepsilon} A_{mn} \beta_x \sin(\beta_x x) \sin(\beta_y y) e^{-j\beta_z z}, \tag{4b}$$

$$E_z = 0, \tag{4c}$$

$$H_x = \frac{1}{\omega\mu\varepsilon} A_{mn} \beta_x \sin(\beta_x x) \sin(\beta_y y) \beta_z e^{-j\beta_z z}, \tag{4d}$$

$$H_y = \frac{-1}{\omega\mu\varepsilon} A_{mn} \cos(\beta_x x)\beta_y \cos(\beta_y y) \beta_z e^{-j\beta_z z}, \tag{4e}$$

$$H_z = \frac{-j}{\omega\mu\varepsilon} A_{mn} \cos(\beta_x x) \sin(\beta_y y) e^{-j\beta_z z} (\beta^2 - \beta_z^2). \tag{4f}$$

The cutoff frequencies of modes TE_{01} and TE_{11}, calculated from

$$(f_c)_{mn} = \frac{c_0}{2\pi\sqrt{\varepsilon_r}} \sqrt{\beta_x^2 + \beta_y^2}, \tag{5}$$

are 2.64 GHz and 5.20 GHz respectively. To corroborate it, an eigenmode simulation of the resonator has been carried out using CST Studio Suite, imposing either electric or magnetic perfect conductor boundary conditions in each of the walls. Fig. 2 shows the analytical and measured electric field inside the resonator for both modes. As it can be seen, there is an excellent agreement between the representation of the analytical equations and the simulation.

B. Top metallized resonator

Based on the DRA analysed above, in this case, the ground plane and the top metallization are considered as PEC, whereas the other walls are still PMC. The boundary conditions are now

$$E_z(x = 0, 0 \le y \le l_y, 0 \le z \le l_z) = 0, \tag{6a}$$

$$E_z(x = l_x, 0 \le y \le l_y, 0 \le z \le l_z) = 0, \tag{6b}$$

$$E_y(x = 0, 0 \le y \le l_y, 0 \le z \le l_z) = 0, \tag{6c}$$

$$E_y(x = l_x, 0 \le y \le l_y, 0 \le z \le l_z) = 0, \tag{6d}$$

$$H_x(0 \le x \le l_x, y = 0, 0 \le z \le l_z) = 0, \tag{6e}$$

$$H_x(0 \le x \le l_x, y = l_y, 0 \le z \le l_z) = 0. \tag{6f}$$

Although the vector potential F_z^+, β_y and the electric and magnetics fields are given by the same expressions, (2), (3b) and (4), the value of β_x is now

$$\beta_x = \frac{m\pi}{l_x}. \tag{7}$$

m can take again values 0,1,2,3 ...

This difference is due to the fact that in this case the parallel walls of the x-axis have the same boundary condition, whereas in the other case the boundary conditions of that axis were different. The cutoff frequencies of modes TE_{01} and TE_{11}, calculated from (5), are now 2.11 GHz and 3.80 GHz respectively. As seen, there is a miniaturization of the electrical size of the resonator. Furthermore, the analytical and simulated field configuration shown in Fig. 2, is more suitable for making a feed though a vertical probe, trying to excite both modes. The electromagnetic simulation corroborates again the good agreement between analytical and simulated electric fields.

III. Assessment by Simulation

Two copper sheets of 1 mm thickness have been adhered to the resonator, that is fed by a current through a vertical probe. The ground plane is welded to the outer contact of a SMA

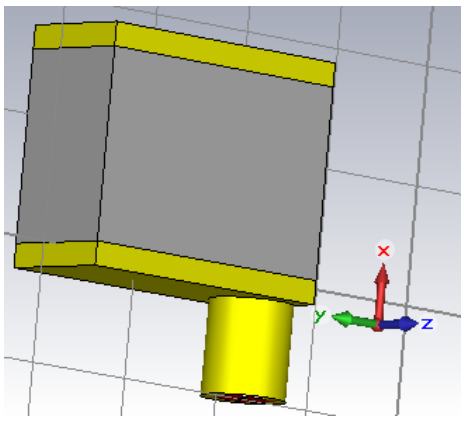

Fig. 3. Geometry of the simulated Dielectric Resonator Antenna.

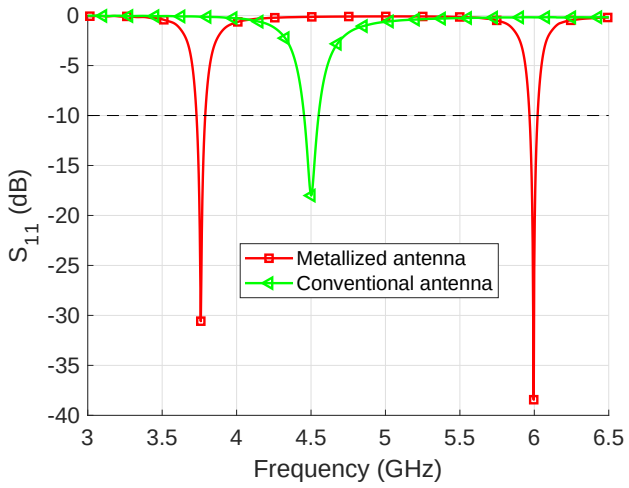

Fig. 4. S_{11} of the conventional and metallized antenna.

connector, whereas the inner contact is extended to be used as a vertical probe. The structure, shown in Fig. 3 has been simulated using the Time Domain Solver of CST Studio Suite. Fig. 4 shows the value of S_{11} parameter of the metallized and non-metallized antennas. From Fig. 4, the resonant frequency of the first mode decreases from 4.5 GHz to 3.75 GHz by adding the metallization. Furthermore, carefully positioning of the probe allows another matched mode (TE_{11}), whose resonant frequency is around 6 GHz. The structure shows ease to be matched and to be use as a dual-band antenna. Its simulated radiation patterns at 3.75 GHz and 6 GHz are shown in Fig. 5, seeing that they are complementary between them, another interesting feature of the designed antenna.

IV. Conclusions

A new technique for miniaturizing rectangular dielectric resonator antennas has been proposed in this paper. A theoretical study has been made to characterize the electromagnetic modes inside the resonator, showing that it is possible to decrease the frequency of the resonator modes just by adding a metallic sheet on top of it. Later, the resonator has been fed by a vertical probe, showing that there is a significant reduction of its electrical size by adding the metallization. Furthermore, a dual-band response, exciting the first two modes of the resonator and complementary radiation patterns

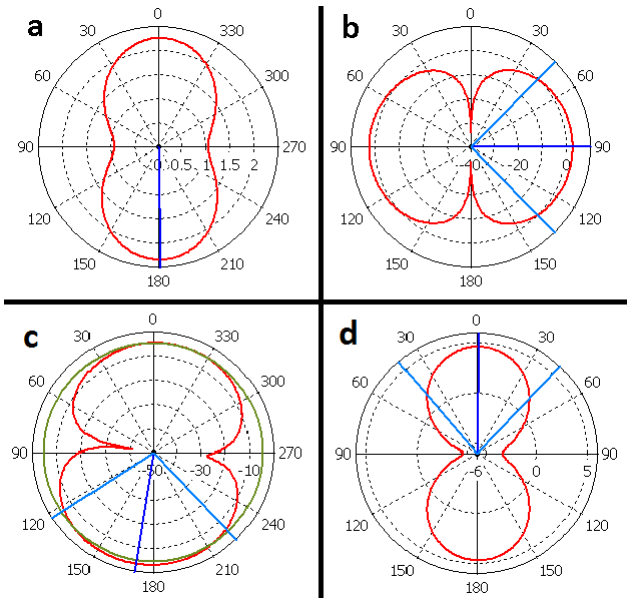

Fig. 5. Simulated radiation patterns of the antenna: (a) at 3.75 GHz and $\theta = 90^o$-plane, (b) at 3.75 GHz and $\phi = 0^o$-plane, (c) at 6 GHz and $\theta = 90^o$-plane and (d) at 6 GHz and $\phi = 0^o$-plane.

of both modes have been obtained. The proposed technology seems a good candidate for dual-band wireless application in future communication devices.

Acknowledgements

This work has been supported by the Spanish Ministerio de Economía, Industria y Competitividad under Project AD-DMATE TEC2016-76070-C3-3-R (AEI/FEDER, UE) and by the Spanish Ministerio de Educación, Cultura y Deporte under Grant FPU16/00246.

References

[1] K. Ali, S. Ali, H. R. Chowdhury and A. Ahmed, "Design and performance analysis of a textile antenna suitable for smart clothing," *2017 IEEE Region 10 Humanitarian Technology Conference (R10-HTC)*, Dhaka, 2017, pp. 367-370.

[2] A. Sabban, "Small wearable antennas for wireless communication and medical systems," *2018 IEEE Radio and Wireless Symposium (RWS)*, Anaheim, CA, USA, 2018, pp. 161-164.

[3] W. Zhefei and F. Jiahui, "A design of miniaturization LPDA antenna with ultra wideband," *2015 IEEE 6th International Symposium on Microwave, Antenna, Propagation, and EMC Technologies (MAPE)*, Shanghai, 2015, pp. 819-821.

[4] M. H. Jamaluddin, N. A. Mohammad and S. Z. Naqiyah, "Size reduction of MIMO Dielectric Resonator Antenna for LTE application," *2016 IEEE Asia-Pacific Conference on Applied Electromagnetics (APACE)*, Langkawi, 2016, pp. 286-290.

[5] K. Yu, Y. Li and Y. Wang, "Multi-band metamaterial-based microstrip antenna for WLAN and WiMAX applications," *2017 International Applied Computational Electromagnetics Society Symposium* - Italy (ACES), Florence, 2017, pp. 1-2.

[6] L. Cheng et al., "Dual-band monopole antenna with multi-band EBG ground plane for 2.4/5 GHz WLAN applications," *2016 IEEE International Conference on Microwave and Millimeter Wave Technology (ICMMT)*, Beijing, 2016, pp. 734-736.

[7] R. D. Richtmyer, "Dielectric resonators," *J. Appl. Phys.*, vol. 10, pp. 391-398, Jun. 1939.

[8] M. W. McAllister, S. A. Long and G. L. Conway, "Rectangular dielectric resonator antenna," in *Electronics Letters*, vol. 19, no. 6, pp. 218-219, March 17 1983.

[9] H. Yuet Yee, "Natural Resonant Frequencies of Microwave Dielectric Resonators (Correspondence)," in *IEEE Transactions on Microwave Theory and Techniques*, vol. 13, no. 2, pp. 256-256, Mar 1965.